Equation of state of low-density neutron matter, and the $^1S_0$ pairing gap

S. Gandolfi and A. Yu. Illarionov*
SISSA, International School of Advanced Studies, via Beirut 2/4, I-34014 Trieste, Italy and INFN, Sezione di Trieste, Trieste, Italy

F. Pederiva
Dipartimento di Fisica, University of Trento, via Sommarive 14, I-38050 Povo, Trento, Italy and INFN, Gruppo collegato di Trento, Trento, Italy

K. E. Schmidt
Department of Physics, Arizona State University, Tempe, Arizona 85287, USA

S. Fantoni
SISSA, International School of Advanced Studies, via Beirut 2/4, I-34014 Trieste, Italy, INFM/CNR-DEMOCRITOS National Simulation Center, Trieste, Italy, and INFN, Sezione di Trieste, Trieste, Italy
(Received 9 July 2009; published 16 October 2009)

We report results of the equation of state of neutron matter in the low-density regime, where the Fermi wave vector ranges from $0.4 \leqslant k_F \leqslant 1.0$ fm^{-1}. Neutron matter in this regime is superfluid because of the strong and attractive interaction in the $^1S_0$ channel. The properties of this superfluid matter are calculated starting from a realistic Hamiltonian that contains modern two- and three-body interactions. The ground state energy and the $^1S_0$ superfluid energy gap are calculated using the auxiliary field diffusion Monte Carlo method. We study the structure of the ground state by looking at pair distribution functions as well as the Cooper-pair wave function used in the calculations.

DOI: 10.1103/PhysRevC.80.045802 PACS number(s): 21.65.Cd, 26.60.−c, 24.10.Cn

I. INTRODUCTION

Pure neutron matter is the natural first approximation to the baryonic matter that composes the bulk of neutron stars. At very low densities below the neutron drip line (i.e., where the Fermi wave vector is roughly, $k_F \lesssim 0.2$ fm^{-1}), neutron star matter is conjectured to be nuclei surrounded by a relativistic gas of electrons [1]. At higher densities, the matter becomes liquid and very neutron rich. Here we study matter at the Fermi wave vector $0.4 \leqslant k_F \leqslant 1.0$ fm^{-1}, where it is reasonable to approximate it as pure neutron matter, and we also extend some of our results into the lower density regime in order to compare them with other calculations.

At these densities, the interaction is dominated by the $^1S_0$ channel with a large and negative scattering length, $a \simeq -18.5$ fm. The product of the effective range and the Fermi wave vector is of order unity, so while the form of interaction cannot be neglected, it becomes less important. Analysis of the phase shifts of the neutron-neutron $^1S_0$ interaction indicates that neutrons should pair and form a superfluid. Therefore the superfluid phase must be included when investigating the equation of state in this regime.

Many methods have been used to approximately calculate the equation of state. One class of methods uses Skyrme or relativistic mean-field methods that use effective interactions that have been fit to the properties of nuclei. However, even those calculations that describe neutron-rich nuclei reasonably well give rather different equations of state for pure neutron matter [2]. We instead use a nonrelativistic Hamiltonian with two- and three-body interactions. All modern accurate two-body interactions fit the Nijmegen data [3] within experimental errors and should give essentially the same equation of state at low density. At longer range, these interactions are dominated by the one-pion exchange and have strong spin-isospin dependence, which must be included for accurate predictions. Three- and higher-body interactions are less well known, but in this density regime they are small.

Our calculations extend the work we first reported in Ref. [4]. The ground state of neutron matter is computed using the auxiliary field diffusion Monte Carlo [5] (AFDMC) algorithm; it is an extension of the diffusion Monte Carlo method [6], and the Green's function Monte Carlo method [7]. These Monte Carlo algorithms are very well suited to projecting a trial wave function onto the ground state in order to study the ground state properties of a system. The Green's function Monte Carlo method has been used to study the properties of light nuclei with very high accuracy [8]. The advantage of the auxiliary field diffusion Monte Carlo method over the Green's function Monte Carlo method is that it can be extended to larger nuclear systems; in fact, it has been used to calculate properties of heavy nuclei [9], neutron-rich isotopes [10,11], and neutron [12,13] and nuclear matter [14] by simulating systems with upward of 100 nucleons.

The equation of state of neutron matter in the low-density regime has been the subject of many previous calculations [4,15–24]. While in this regime, different Hamiltonians and different methods give similar behaviors for the energy as a function of the density, there are appreciable differences in other important properties. In particular, the value of the

*Current address: Dipartimento di Fisica, University of Trento, via Sommarive 14, I-38050 Povo, Trento, Italy.

$^1S_0$ superfluid energy gap is at present not well clarified and strongly depends on the Hamiltonian and the solution method [4]. In this paper, we focus on both the energy and the energy gap by considering a fully realistic Hamiltonian, and solve for the ground state using the AFDMC technique. As a starting point for the calculation, we considered two forms for the trial wave function. The first is a filled Fermi sea having the properties of a normal Fermi liquid, which we will call the normal phase. The second has neutrons paired in the $^1S_0$ channel with a Bardeen-Cooper-Schrieffer (BCS) superfluid structure [25]. At a fixed density, we find that the superfluid phase of the system is only marginally favored over the normal phase. However, to calculate the superfluid energy gap, the BCS structure must be used.

II. HAMILTONIAN

We study the ground state of neutron matter beginning with the nonrelativistic nuclear Hamiltonian

$$H = -\frac{\hbar^2}{2m}\sum_{i=1}^{N}\nabla_i^2 + \sum_{i<j} v_{ij} + \sum_{i<j<k} V_{ijk}, \tag{1}$$

where m is the mass of the neutron, and v_{ij} and V_{ijk} are two- and three-body potentials. Such a form for the Hamiltonian (with the kinetic energy modified to take into account the mass difference of the neutron and proton) has been shown to describe properties of light nuclei in good agreement with experimental data (see Ref. [8] and references therein). All the degrees of freedom responsible for the interaction between nucleons (such as the π, ρ, Δ, etc.) are integrated out and included in v_{ij} and V_{ijk}.

At present, several realistic two-nucleon interactions fit the scattering data with very high precision. We use the two-nucleon potentials belonging to the Argonne family [26]. Such interactions are written as

$$v_{ij} = \sum_{p=1}^{M} v_p(r_{ij})O^{(p)}(i,j), \tag{2}$$

where $O^{(p)}(i,j)$ are spin-isospin-dependent operators. The number of operators M characterizes the interaction; the most accurate for the Argonne family is the Argonne AV18 with $M = 18$ [26]. Here we consider a simpler form derived from AV18, namely, the AV8′ [27] with a smaller number of operators. For many systems, the difference between this simpler form and the full AV18 potential can be computed perturbatively [13,28], as has been done in all Green's function Monte Carlo calculations to date. Most of the contribution of the two-nucleon interaction is due to one-pion exchange between nucleons, but the effect of other meson exchanges as well as some phenomenological terms are also included.

The eight $O^{(p)}(i,j)$ operators in AV8′ are given by the four central components $\mathbf{1}$, $\boldsymbol{\tau}_i\cdot\boldsymbol{\tau}_j$, $\boldsymbol{\sigma}_i\cdot\boldsymbol{\sigma}_j$, $(\boldsymbol{\sigma}_i\cdot\boldsymbol{\sigma}_j)(\boldsymbol{\tau}_i\cdot\boldsymbol{\tau}_j)$, the tensor S_{ij}, the tensor-τ component $S_{ij}\boldsymbol{\tau}_i\cdot\boldsymbol{\tau}_j$ [where $S_{ij} = 3(\boldsymbol{\sigma}_i\cdot\hat{r}_{ij})(\boldsymbol{\sigma}_j\cdot\hat{r}_{ij}) - \boldsymbol{\sigma}_i\cdot\boldsymbol{\sigma}_j$], the spin-orbit $\boldsymbol{L}_{ij}\cdot\boldsymbol{S}_{ij}$, and the spin-orbit-$\tau$ $(\boldsymbol{L}_{ij}\cdot\boldsymbol{S}_{ij})(\boldsymbol{\tau}_i\cdot\boldsymbol{\tau}_j)$ [where $\boldsymbol{L}_{ij}$ and $\boldsymbol{S}_{ij}$ are the relative angular momentum and the total spin of the pair ij]. All the parameters describing the radial functions of each operator in AV18 are fit to nucleon-nucleon scattering data below 350 MeV in the Nijmegen database [3]. The AV8′ interaction is obtained by starting from AV18 and making an isoscalar projection. It is refit in order to keep the most important features of AV18 in the scattering data and the properties of the deuteron [27].

The three-nucleon interaction is essential to overcome the underbinding of nuclei with more than two nucleons. While the two-nucleon interaction is fit to scattering data and correctly gives the deuteron binding energy, it is not sufficient for describing the ground state of light nuclei with three or more nucleons. The Urbana-IX (UIX) potential corrects this and was fit to obtain the correct triton energy using Green's function Monte Carlo and to correctly reproduce the expected saturation energy of nuclear matter within the Fermi hypernetted-chain approximation [29]. It contains a Fujita-Miyazawa term [30] that describes the exchange of two pions between three nucleons, with the creation of an intermediate excited Δ state. Again, a phenomenological part is added to sum all the other neglected terms. The generic form of UIX is

$$V_{ijk} = V_{2\pi} + V_R. \tag{3}$$

The Fujita-Miyazawa term [30] is spin-isospin dependent:

$$V_{2\pi} = A_{2\pi}\sum_{cyc}\Big[\{X_{ij},X_{jk}\}\{\boldsymbol{\tau}_i\cdot\boldsymbol{\tau}_j,\boldsymbol{\tau}_j\cdot\boldsymbol{\tau}_k\} + \frac{1}{4}[X_{ij},X_{jk}][\boldsymbol{\tau}_i\cdot\boldsymbol{\tau}_j,\boldsymbol{\tau}_j\cdot\boldsymbol{\tau}_k]\Big], \tag{4}$$

where the X_{ij} operators describe the one-pion exchange (see Ref. [31] for details). The phenomenological part of UIX is

$$V_{ijk}^R = U_0\sum_{cyc} T^2(m_\pi r_{ij})T^2(m_\pi r_{jk}). \tag{5}$$

The factors $A_{2\pi}$ and U_0 are kept as fitting parameters. Other forms of three-nucleon interaction, called the Illinois forces [31], which include three-nucleon Feynman diagrams with two-Δ intermediate states, are available. Unfortunately they provide unrealistic overbinding of neutron systems when the density increases [12,32], and they do not seem to describe realistically the higher density (i.e., $\rho \geqslant \rho_0 = 0.16$ fm^{-3}) nucleonic systems. However, in the low-density regime considered in this paper, the contribution of the three-body interaction is very small compared to the total energy of the system, so the small errors in the UIX interaction should have negligible contributions to the equation of state and energy gap.

III. AFDMC METHOD AND THE PFAFFIAN WAVE FUNCTION

Uniform neutron matter is simulated by solving the ground state of a fixed number N of neutrons in a periodic box, whose volume is fixed by the density of the system. The ground state of the system is calculated by means of the AFDMC algorithm [5]. Diffusion Monte Carlo projects out the lowest energy state from a trial wave function ψ_T by a propagation in imaginary time:

$$\psi(\tau) = e^{-(H-E_T)\tau}\psi_T, \tag{6}$$

where E_T is a normalization factor. In the $\tau\to\infty$ limit, the only component of ψ_T that survives is the lowest energy one

not orthogonal to ψ_T:

$$\phi_0 = \lim_{\tau\to\infty} \psi(\tau). \tag{7}$$

The evolution in imaginary time is performed by solving the integral equation

$$\psi(R,\tau) = \int dR' G(R,R',\tau)\psi_T(R'), \tag{8}$$

where $G(R,R',\tau)$ is the Green's function of the Hamiltonian that contains a diffusion term, coming from the kinetic operator in H, and a branching term from the potential. The exact form of $G(R,R',\tau)$ is unknown, but it can be accurately approximated in the limit of $\Delta\tau \to 0$. The above integral equation is then solved iteratively, with a small time step, for a sufficiently large number of steps. A detailed description of the algorithm as well as the importance sampling technique used to reduce the variance can be found in Refs. [33,34].

The presence of spin operators in the Hamiltonian requires a summation of all possible good spin states in the wave function [35]. This summation grows exponentially with the number of neutrons; for example, for a system of 14 neutrons, the computation of $\langle\psi(R)|\psi(R)\rangle$ is a sum of squares of 2^{14} spin amplitudes. The explicit summation of spin states is performed in Green's function Monte Carlo, but not in AFDMC, calculations where the spin states are sampled using Monte Carlo techniques [5]. This sampling is performed by reducing the quadratic dependence of spin operators in the exponential to a linear form by means of the Hubbard-Stratonovich transformation. The effect of an exponential of a linear combination of spin operators consists of a rotation of the spinor for each neutron during the propagation. To have an efficient algorithm, the trial function must be chosen so that it can be efficiently evaluated when each neutron is in a specific position and spinor state.

Since both positions and spins can be sampled, the AFDMC method can be used to solve for the ground state of much larger systems (over 100 neutrons) than the Green's function Monte Carlo with full spin summations.

More detailed explanations of the AFDMC method and how to include the full two- and three-nucleon interactions in the propagator can be found in Refs. [12,13,32,36], where the fixed-phase approximation used to control the fermion sign problem is also discussed.

The AFDMC method projects out the lowest energy state with the same symmetry as the trial wave function from which the projection is started. The general form of the trial wave function is

$$\psi_T(R,S) = \left[\prod_{i<j} f_J(r_{ij})\right] \Phi(R,S), \tag{9}$$

where $R \equiv (\boldsymbol{r}_1,\ldots,\boldsymbol{r}_N)$ represents the spatial coordinates and $S \equiv (s_1,\ldots,s_N)$ the spin states of the neutrons. The spin assignments s_i consist of giving the two spinor components for each neutron, namely, the two complex numbers a_i, b_i where

$$|s_i\rangle = a_i|\uparrow\rangle + b_i|\downarrow\rangle, \tag{10}$$

and the $\{|\uparrow\rangle, |\downarrow\rangle\}$ is the spin-up and spin-down basis. The function f_J entering in the so-called Jastrow part of the trial wave function has only the role of reducing the overlap of neutrons and thereby reducing the energy variance. Since it does not change the phase of the wave function, it does not influence the computed energy value in projection methods. The function f_J is computed as described in Ref. [13].

The antisymmetric part Φ of the trial wave function is usually given by the ground state of noninteracting fermions (Fermi gas), which is written as a Slater determinant of single-particle functions. For example, homogeneous systems are usually simulated by considering plane waves as orbitals. In this case,

$$\Phi_n(R,S) = \mathcal{A}\left[\phi_1(\boldsymbol{r}_1,s_1)\ldots\phi_N(\boldsymbol{r}_N,s_N)\right], \tag{11}$$

where $\mathcal{A}$ is the antisymmetrizer [see Eq. (A3)],

$$\phi_\alpha(\boldsymbol{r}_i,s_i) = e^{i\boldsymbol{k}_\alpha\cdot\boldsymbol{r}_i}\langle s_i|\chi_{s,m_s,\alpha}\rangle, \tag{12}$$

and α is the set of quantum numbers of single-particle orbitals that are plane waves fitting the box. The correct symmetry of the ground state is given using the closed shells occurring when the total number of fermions in a particular spin configuration is 1, 7, 19, 27, 33, ...

However, in superfluid neutron matter, there is a strong coupling between neutrons, and a wave function having a BCS structure must be used.

BCS pairing correlations can substantially change the nodal structure of a trial wave function [37,38]. This change, which gives the off-diagonal long-range order of the superfluid phase, will greatly alter the fixed-phase (or constrained path) energy. To correctly describe the superfluid ground state with these quantum Monte Carlo methods, we need to use a trial wave function with explicit pairing. For central potentials and singlet pairing, the BCS trial function can be written as a determinant [37,39]. However, for problems with a tensor force, or for spin triplet pairing, a general pairing state must be used.

A fully paired state of N neutrons can be written, as shown in Appendix A, as

$$\mathcal{A}[\phi_{12}\phi_{34}\ldots\phi_{N-1,N}]. \tag{13}$$

Similarly, we can construct a general state with n paired and o unpaired orbitals for a total of $N = 2n + o$ particles as

$$\mathcal{A}[\phi_{12}\phi_{34}\ldots\phi_{2n-1,2n}\ldots\psi_1(2n+1)\ldots\psi_o(N)], \tag{14}$$

which is the Pfaffian of the $(N+o)\times(N+o)$ skew-symmetric matrix [39]

$$\begin{pmatrix}
0 & \phi_{12} & \phi_{13} & \ldots & \phi_{1N} & \psi_1(1) & \ldots & \psi_o(1) \\
-\phi_{12} & 0 & \phi_{23} & \ldots & \phi_{2N} & \psi_1(2) & \ldots & \psi_o(2) \\
\vdots & \vdots & \ddots & \vdots & \vdots & \vdots & \vdots & \vdots \\
-\phi_{1N} & -\phi_{2N} & -\phi_{3N} & \ldots & 0 & \psi_1(N) & \ldots & \psi_o(N) \\
-\psi_1(1) & -\psi_1(2) & -\psi_1(3) & \ldots & -\psi_1(N) & 0 & \ldots & 0 \\
\vdots & \vdots & \vdots & \vdots & \vdots & \vdots & \ddots & \vdots \\
-\psi_o(1) & -\psi_o(2) & -\psi_o(3) & \ldots & -\psi_o(N) & 0 & \ldots & 0
\end{pmatrix}, \tag{15}$$

where the lower $o\times o$ section is all zeros.

The Pfaffian is the antisymmetric product

$$\mathrm{Pf}A = \mathcal{A}[a_{12}a_{34}a_{56}\ldots a_{N-1,N}]. \tag{16}$$

The result is normalized such that every equivalent term occurs only once, and $a_{ij} = -a_{ji}$.

Just as the determinant of a dense matrix can be calculated efficiently in order N^3 operations, similar elimination methods can compute the Pfaffian. The basic Pfaffian calculational methods we use here and have used for all previous superfluid neutron matter studies [4,40] are described in some detail in Sec. II of Ref. [41], and those results are summarized in Appendix B along with some additional techniques needed for these nuclear calculations.

The nuclear Hamiltonian has spin-dependent terms that can flip the spin. For the simpler case of a purely central potential, the Hamiltonian will not change the particles' spin. Therefore in this simpler case, we can solve for the ground state in one sector where each particle has a specified spin, and we only need to antisymmetrize over the particles with the same spin. In that case, Φ_{BCS} reduces to a determinant. Since in our AFDMC method, the Hamiltonian can change the particles' spin, and the particles can then take on any spinor value, we need to be able to evaluate the trial wave function for arbitrary spinor values for each particle. Therefore the Pfaffian that gives the full antisymmetric form must be used. As shown in Appendix A, the pairing orbitals ϕ we used have the form

$$\begin{aligned}\phi(\boldsymbol{r}_{ij}, s_i, s_j) &= \sum_{\alpha} \frac{v_{k_\alpha}}{u_{k_\alpha}} e^{i\boldsymbol{k}_\alpha\cdot\boldsymbol{r}_{ij}}\chi(s_i, s_j) \\ &= \sum_{\alpha} c_\alpha e^{i\boldsymbol{k}_\alpha\cdot\boldsymbol{r}_{ij}}\chi(s_i, s_j),\end{aligned} \tag{17}$$

where the sum over α indicates the k-space shells of the cube with $\boldsymbol{k}$ values

$$k_{n_x n_y n_z} = \frac{2\pi}{L}(n_x\hat{\boldsymbol{x}} + n_y\hat{\boldsymbol{y}} + n_z\hat{\boldsymbol{z}}) \tag{18}$$

for integer n_x, n_y, and n_z. The function χ is the spin-singlet wave function for two neutrons

$$\chi(s_i, s_j) = \frac{1}{\sqrt{2}}(\langle s_i s_j|\uparrow\downarrow\rangle - \langle s_i s_j|\downarrow\uparrow\rangle). \tag{19}$$

With the spin states given as spinors as in Eq. (10), this becomes

$$\chi(s_i, s_j) = \frac{a_i^* b_j^* - b_i^* a_j^*}{\sqrt{2}}. \tag{20}$$

Note that if the pairing coefficients c_α are zero for all $|\boldsymbol{k}_\alpha| > k_F$, the Pfaffian of Eq. (15) is exactly the Slater determinant of spin-up and -down neutrons filling the Fermi sea, and the Pfaffian form goes over to the normal liquid state. The parameters c_α are chosen variationally by performing a correlated basis function calculation [40,42]. However, various other wave functions were considered to ascertain the effect of a particular choice on the results.

TABLE I. AFDMC energies per particle for 66 neutrons interacting with the AV8′ + UIX interaction in a periodic box as a function of the Fermi wave vector and corresponding density ρ. The values E_n correspond to the simulation of neutron matter using the Fermi gas ground state in the trial wave function, while E_{BCS} are the results obtained using Φ_{BCS}. All the energies are expressed in MeV.

k_F (fm^{-1})	ρ (fm^{-3})	E_n/N	E_{BCS}/N
0.4	0.00216	1.289(2)	1.239(2)
0.6	0.00730	2.606(4)	2.579(2)
0.8	0.01729	4.277(7)	4.305(3)
1.0	0.03377	6.197(2)	6.231(3)

IV. RESULTS

A. Equation of state

We computed the energy of neutron matter by simulating neutrons in a periodic box at densities corresponding to $k_F = 0.4, 0.6, 0.8$, and 1.0 fm^{-1} using in the trial wave function both Φ_n and Φ_{BCS}. We found that the absolute energy is slightly different depending on the choice of the trial function Φ. The results obtained using the two different trial wave functions are reported in Table I. As can be seen, the BCS state is favored at $k_F = 0.4$ and 0.6 fm^{-1}, while the normal state trial function gives the lowest energy at $k_F = 0.8$ and 1.0 fm^{-1}. The maximum difference between the results for the two different trial wave functions is about 4% of the total energy at $k_F = 0.4$ fm^{-1}, probably because at such a low density the pairing between neutrons in the $^1S_0$ channel is very important, and Φ_{BCS} includes such correlations in the wave function in a more effective way. In the other cases, the energies obtained with Φ_{BCS} and Φ_n are within 1%.

Since the coefficients entering in Φ_{BCS} were chosen by a correlated basis function (CBF) calculation that adds a two-body correlation factor to the usual BCS state [40,42], to determine if this method is adequate for finding a good BCS form, we repeated some of the calculations using different coefficients. In particular, we tried using as a pairing function the solution from the uncorrelated BCS equation, as well as a pairing function with the same form as that of Refs. [22,43]. This calculation has carefully optimized coefficients, but the interaction is the $^1S_0$ channel of AV18 acting only between unlike spins. In both cases, we find the energy is slightly higher than that found when using the correlated basis function coefficients.

The equation of state of low-density neutron matter computed using Φ_{BCS} is displayed in Fig. 1 and compared with the diffusion Monte Carlo results of Gezerlis and Carlson [22], the variational cluster summation calculation of Friedman and Pandharipande [15] and the results of Epelbaum, Krebs, Lee, and Meissner [21]. The differences between the various calculations are due to the different approximations and interactions used. The AFDMC method uses a realistic Hamiltonian containing a modern two-body and the corresponding three-body force. The variational cluster summation calculation was performed using the older Urbana v_{14} two-nucleon interaction [44] modified to include a density-dependent term that models the effect of a three-body force. As mentioned above, the

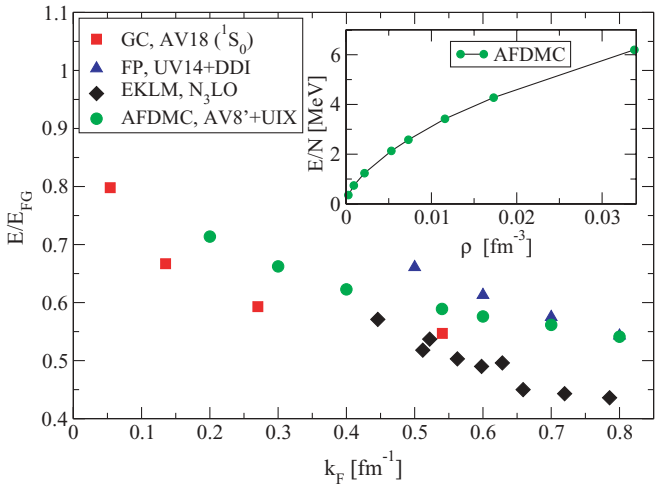

FIG. 1. (Color online) Equation of state of neutron matter as a function of the Fermi wave vector k_F. The energy has been divided by the energy of the noninteracting Fermi gas, $E_{\rm FG} = \frac{3}{5}\frac{\hbar^2 k_F^2}{2m}N$. The AFDMC result is obtained using the full Hamiltonian AV8′ + UIX (green circles), and compared with the results of Gezerlis and Carlson (red squares) who considered a simpler Hamiltonian [22]. The blue triangles correspond to the calculation of Friedman and Pandharipande using the Urbana v_{14} two-nucleon interaction modified to include some three-body effects [15]. The black diamonds show the results of Epelbaum, Krebs, Lee and Meißner [21]. In the inset box, the AFDMC energy in MeV is shown as a function of the density ρ in fm^{-3} along with a curve to guide the eye.

calculation of Gezerlis and Carlson uses only the $^1S_0$ channel interaction of AV18 between unlike spins. This choice is motivated by the fact that this channel is dominant in neutron matter in this regime. However, the effect of other channels as well as using the $^1S_0$ interaction partly in the triplet channel, since all unlike spin pairs interact, could play an important role in the many-body correlations of the system. Finally, Epelbaum and collaborators computed the equation of state within the chiral effective field theory by simulating neutrons on the lattice up to the next-to-next-to-next-to leading order (N$_3$LO) [21].

Each of these calculations used different methods to solve for the ground state. Both the AFDMC and the diffusion Monte Carlo method used by Gezerlis and Carlson are projection methods that, apart from the constraint used to control the fermion sign problem, are exact. However, the constraint plays an important role in finding the correct ground state, and different trial functions give different constraints and therefore different results. For these two Monte Carlo methods, trial functions have the same kind of BCS form. However, Gezerlis and Carlson use a different approach for the choice of the coefficients entering in the pairing orbitals of Eq. (17). Their c_α parameters are chosen by varying them to minimize the fixed-node energy [22,37,38]. Unfortunately, this same technique is not currently applicable to AFDMC because the variance of the calculation is too high to be able to choose the coefficients in a reasonable amount of computational time. The c_α used in our AFDMC calculations are chosen instead by using a correlated BCS wave function solved within the CBF/BCS theory [40,42] as discussed above. The variational cluster summation calculation may suffer from important uncontrolled approximations coming from the cluster expansion, as we recently pointed out in our paper comparing the equation of state of neutron matter at higher densities [13]. In addition, the variational cluster summation calculation does not include any pairing correlations in the variational wave function. The equation of state can be computed using N$_3$LO as described in Refs. [19–21], and the results are available for a small number of neutrons ($N = 12$). They predict an equation of state that is globally lower than the other results. This model, while very promising because it attacks the problem from a more fundamental point of view, will need to be extended to larger systems.

B. Superfluid gap

In a full many-body calculation, the superfluid gap can be evaluated by using the difference

$$\Delta(N) = E(N) - \tfrac{1}{2}\left[E(N+1) + E(N-1)\right], \qquad (21)$$

where the number of neutrons N is taken to be odd. The AFDMC algorithm can be used to simulate very large systems with up to a hundred nucleons [12–14,32]. Unfortunately, because the gap has to be evaluated as the difference between total energies of different systems, the statistical error related to Δ is proportional to the number of neutrons, and we have not been able to develop an efficient method of correlated sampling. As a consequence, in principle, the number of neutrons is arbitrary, but if N is too large, the statistical error affecting the gap becomes larger than the gap itself. The maximum number of neutrons used in this work is 68.

Particular care was taken to check that the AFDMC had converged. The simulations were repeated with different time steps. Neither the energy nor the gap is dependent on the time step used; the extrapolation to the zero limit is within our error bars.

The gap is strongly dependent on the number of neutrons for small N. For both $k_F = 0.4$ and 0.6 fm^{-1}, the Δ computed with $N = 12, \ldots, 18$ is noticeably larger than that computed with $N = 62, \ldots, 68$. We find that at $k_F = 0.4$ fm^{-1}, the gap is $\Delta(14) = 1.79(6)$ and $\Delta(66) = 1.5(2)$ MeV; while at $k_F = 0.6$ fm^{-1}, $\Delta(14) = 2.59(6)$ and $\Delta(66) = 2.1(2)$ MeV. This behavior is well described by the analysis of Gezerlis and Carlson, who solved the BCS equation in the simulation cell and then reproduced this effect by using diffusion Monte Carlo [22]. In their paper, they calculate with up to 90 particles without observing a substantial change in the gap compared to that given by simulating the system with about 66 particles, giving us confidence that our gaps have converged.

We report in Fig. 2 the superfluid gap computed with AFDMC using $N = 62, \ldots, 68$, compared with other calculations. It is clear that the different methods used to compute the pairing gap give different results. The mean-field BCS result is essentially unchanged when other realistic two-nucleon interactions are used [42,51], and it reaches a maximum of about 3 MeV. This is because all the two-body interactions

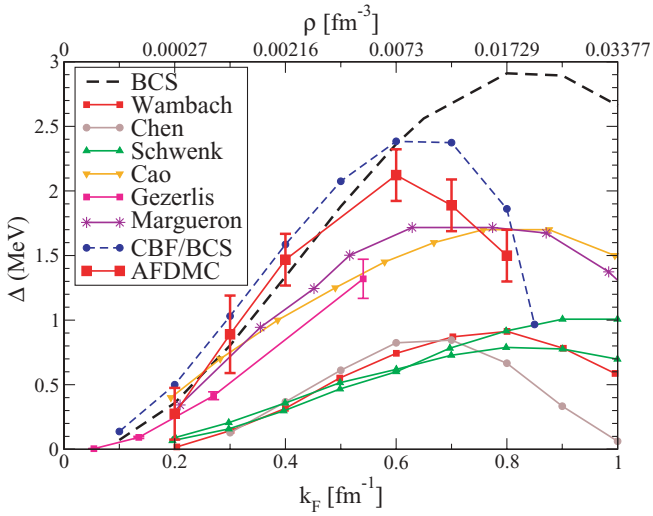

FIG. 2. (Color online) $^1S_0$ pairing gap of neutron matter as a function of the Fermi wave vector k_F computed with different methods. In the figure we display works of Wambach *et al.* [45], Chen *et al.* [46], Schulze *et al.* [47], Schwenk *et al.* [48], Cao *et al.* [49], Gezerlis and Carlson [22], and Margueron *et al.* [50]. All the results are compared with a BCS calculation (dashed line).

are fit by reproducing the S- and P-wave components from experimental data. However, a realistic study of the pairing gap must include the corrections due to the polarization effects given by the medium. The various results can be essentially divided into two different groups according to the different way used to include this effect: (1) the many-body calculation using effective interactions based on Brueckner theory or Hartree-Fock calculations or (2) the microscopic calculations (Monte Carlo methods or CBF theory) where the whole Hamiltonian describing the system is solved. The many-body effective-interaction calculations of Wambach *et al.* [45], Chen *et al.* [46], Schulze *et al.* [47] and Schwenk *et al.* [48] predict a large reduction compared to the BCS gap, with a maximum gap of about 1 MeV. The microscopic calculations based on CBF theory or using quantum Monte Carlo techniques show a reduction of the gap compared to the BCS result particularly at high densities, where the maximum is about 2.1 MeV using AFDMC and 2.4 MeV with correlated basis functions. The other available quantum Monte Carlo result by Gezerlis and Carlson was performed for smaller densities, because it neglects several contributions from other channels of the interaction [22]. The recent results provided by other many-body techniques using Bruckner Hartree-Fock and new effective interactions by Cao *et al.* [49] and Margueron *et al.* [50] predict a superfluid gap closer to the AFDMC result. Their maximum value of Δ is about 1.7 MeV. In addition, the different methods predict different densities at which the gap reaches the maximum value.

C. Pair distribution functions and pairing orbitals

Besides computing energies, the structure of $^1S_0$ pairing can be investigated by a qualitative study of pair distribution functions. If the pair energy is low enough that only the $^1S_0$ or the $^1S_0$ and $^3P_1$ channels are important, the interaction can be written as $v_c(r_{ij}) + v_\sigma(r_{ij})\boldsymbol{\sigma}_i \cdot \boldsymbol{\sigma}_j$. Even though we keep the full interaction, it is interesting to look at the two-body distributions that have this form. The corresponding pair distribution functions are defined by

$$g_c(r) = \frac{1}{2\pi r^2 \rho N} \sum_{i<j} \frac{\langle \psi | \delta(r_{ij} - r) | \psi \rangle}{\langle \psi | \psi \rangle}, \tag{22}$$

and

$$g_\sigma(r) = \frac{1}{2\pi r^2 \rho N} \sum_{i<j} \frac{\langle \psi | \delta(r_{ij} - r) \boldsymbol{\sigma}_i \cdot \boldsymbol{\sigma}_j | \psi \rangle}{\langle \psi | \psi \rangle}, \tag{23}$$

where ρ is the density. $\rho g_c(r) d^3r$ is the probability of finding a neutron in an infinitesimal volume d^3r at a distance r from another neutron, while $\rho g_\sigma(r) d^3r$ is -3 times the probability of finding a neutron such that the two are in a singlet state plus the probability of finding a neutron such that the two are in a triplet state. In the limit of large r, $g_c(r) \to 1$, while $g_\sigma(r) \to 0$.

Since $\boldsymbol{\sigma}_i \cdot \boldsymbol{\sigma}_j$ is 1 in triplet and -3 in singlet channels, we can write singlet and triplet pair distribution functions, $g_S(r)$, where $S = 0$ for the singlet and $S = 1$ for the triplet,

$$g_0(r) = \tfrac{1}{4}[g_c(r) - g_\sigma(r)], \tag{24}$$

and

$$g_1(r) = \tfrac{1}{4}[3g_c(r) + g_\sigma(r)]. \tag{25}$$

Because AFDMC, like diffusion Monte Carlo, most easily calculates mixed estimates

$$\langle O \rangle_M = \frac{\langle \psi | O | \psi_T \rangle}{\langle \psi | \psi_T \rangle}, \tag{26}$$

we extrapolate these from the variational values

$$\langle O \rangle_V = \frac{\langle \psi_T | O | \psi_T \rangle}{\langle \psi_T | \psi_T \rangle} \tag{27}$$

as $\langle O \rangle \simeq 2\langle O \rangle_M - \langle O \rangle_V$.

The pair distribution functions computed with AFDMC are shown in Fig. 3. Closed symbols refer to $g_c(r)$ at various densities, while open symbols represent $g_\sigma(r)$. The calculations were performed at different Fermi wave vectors, as indicated in the legend of the figure. As can be seen, the strong interaction in the $^1S_0$ channel is evident in both the $g_c(r)$ and $g_\sigma(r)$, which exhibit peaks at the same distance. The peak value of $g_\sigma(r)$ is about -3 times that of $g_c(r)$, and the peaks increase as the density is lowered.

The strong $^1S_0$ correlation is more evident using the singlet and triplet channel distribution functions, which we show in Fig. 4. Closed symbols represent the singlet state of the pair, while open ones the triplet state at various Fermi wave vectors as indicated in the legend. The singlet channel becomes very strong and dominant when the density decreases.

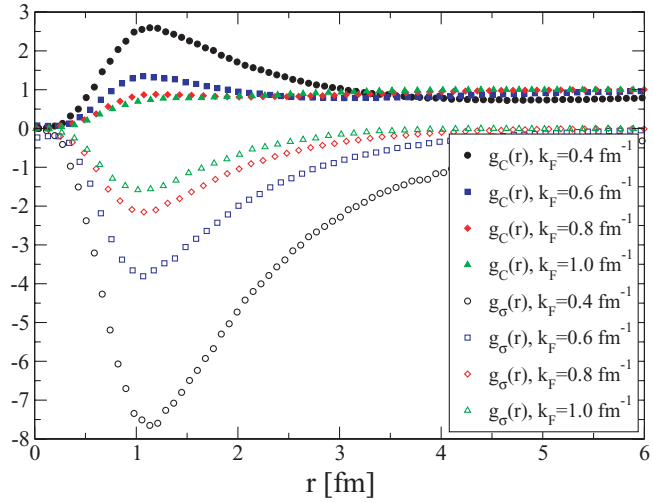

FIG. 3. (Color online) Pair distribution functions $g_c(r)$ and $g_\sigma(r)$ for neutron matter as defined in the text. The curves with closed symbols are the $g_c(r)$, those with open ones indicate $g_\sigma(r)$, corresponding to different Fermi wave vectors. See the text for details.

We can compare these pair distribution functions with those of a noninteracting Fermi gas,

$$g_0^{\mathrm{FG}}(r) = \tfrac{1}{4}[1 + l^2(r)], \tag{28}$$

and

$$g_1^{\mathrm{FG}}(r) = \tfrac{3}{4}[1 - l^2(r)], \tag{29}$$

where $l(r)$ is the Slater function defined as

$$l(r) = 3\frac{\sin(k_F r) - k_F r \cos(k_F r)}{(k_F r)^3}. \tag{30}$$

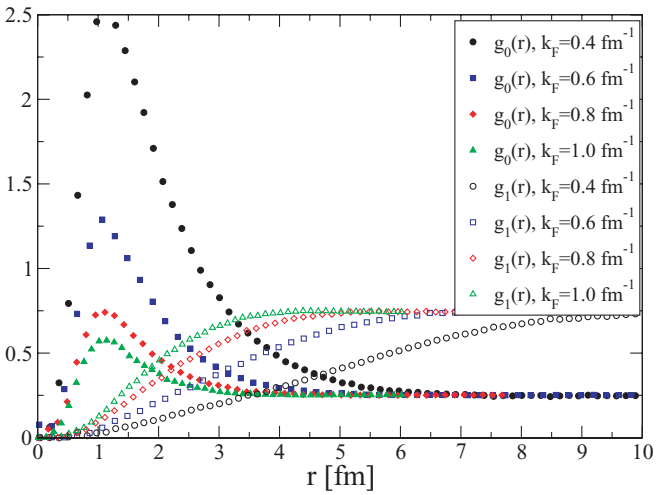

FIG. 4. (Color online) Pair distribution functions $g_0(r)$ and $g_1(r)$ as defined in the text. Closed symbols represent the pair distribution function projected into the singlet spin channel, while open ones the triplet spin channel. See the text for details.

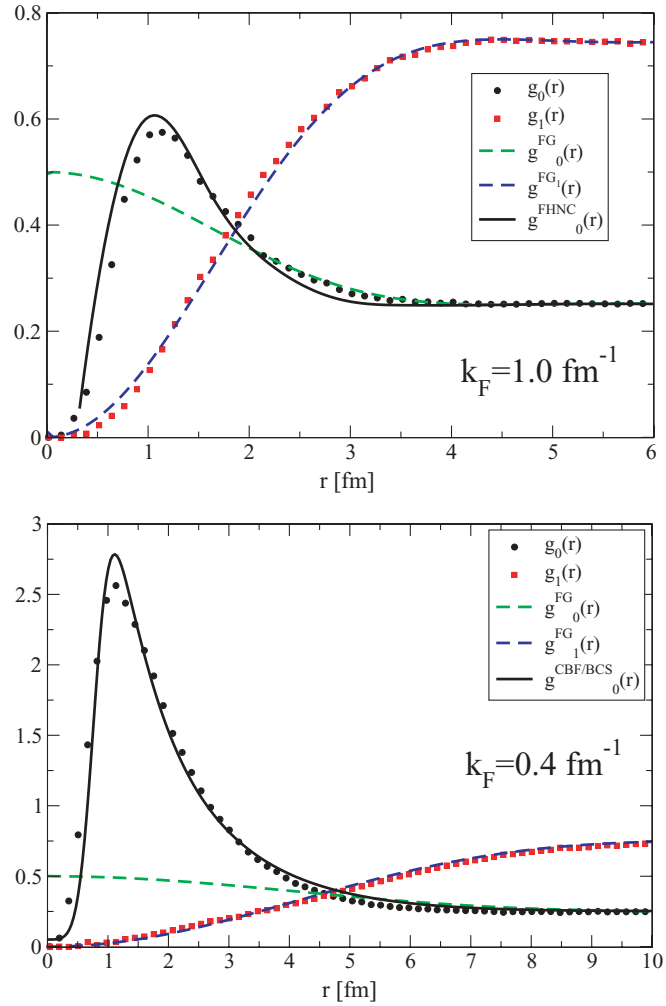

FIG. 5. (Color online) Pair distribution functions $g_0(r)$ and $g_1(r)$, as defined in the text, at $k_F = 1.0$ fm^{-1} and $k_F = 0.4$ fm^{-1}. See the text for details.

We report in Fig. 5, $g_0(r)$ and $g_1(r)$ and the corresponding $g_0^{\mathrm{FG}}(r)$ and $g_1^{\mathrm{FG}}(r)$ of the Fermi gas at Fermi wave vectors $k_F = 1.0$ and $k_F = 0.4$ fm^{-1}. The triplet pair distribution function does not differ very much from the noninteracting case; it does have a small deviation at large distances for $k_F = 1.0$ fm^{-1}. This means that quantum correlations, in this channel and in this density regime, are not too important. They become relatively more important at higher densities. The singlet pair distribution function, instead, is completely different from that of the noninteracting Fermi gas. However, at $k_F = 1.0$ fm^{-1}, the peak of $g_0(r)$ is not so very far from the maximum value of $g_0^{\mathrm{FG}}(r)$ at the origin; while at $k_F = 0.4$ fm^{-1}, the strong peak of the singlet is far from the noninteracting case. In Fig. 5, the singlet pair distribution function is also compared with the corresponding variational correlated basis function calculations using either the Fermi hyper-netted chain (FHNC) approach [52] for the normal phase or CBF/BCS [42] for the superfluid phase. It is evident that the strong peak of the singlet is due to the presence of the strong correlations in the system.

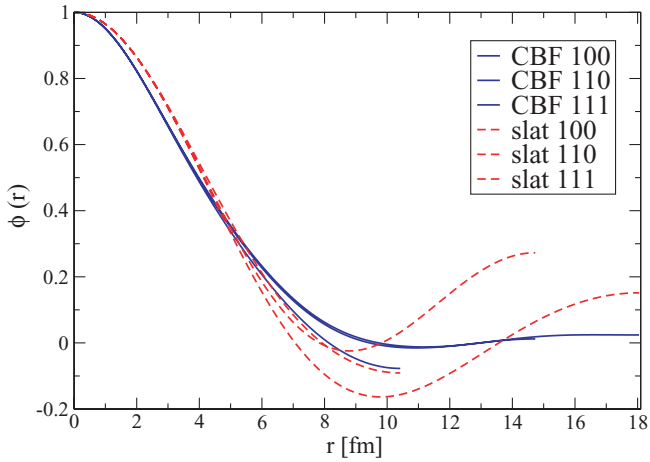

FIG. 6. (Color online) Spatial functions used in the pairing orbitals at $k_F = 0.6$ fm^{-1}. The solid (blue) line is the function obtained using the correlated basis function (CBF) coefficients, while the dashed (red) line is the simulation cell Slater function.

We plot in Fig. 6 the spatial part of the pairing function used in $\Phi_{\rm BCS}$ at $k_F = 0.6$ fm^{-1}, along the three spatial directions 100, 110, and 111 obtained by using the CBF coefficients. These are compared with the simulation cell Slater functions $\ell_{\rm cell} = \frac{2}{N}\sum_{\boldsymbol{k},k<k_F} e^{i\boldsymbol{k}\cdot\boldsymbol{r}}$. The functions corresponding to each direction end at $L/2$, $L/\sqrt{2}$, and $\sqrt{3/4}L$, where L is the side of the simulation cell.

V. CONCLUSION

We have reported a detailed computation of the equation of state of neutron matter in the low-density regime where the system is superfluid and neutrons pair in the $^1S_0$ channel. The superfluid gap was also computed. The presence of spin-dependent interactions means that the wave function must be written as a Pfaffian of two-neutron pairing orbitals, and the definition and the computation of the Pfaffian was also discussed.

The use of a realistic nuclear Hamiltonian without using any effective interaction combined with the use of a very accurate projection technique makes these results a benchmark for other methods. Because of the constraint used to control the fermion sign problem, the results could in principle depend on the importance function. We carefully verified the effect of the wave function without observing a particular bias due to the fixed-phase constraint used in the calculations.

We compared the computed equation of state with other results, and we observed important deviations that could be due both to the model Hamiltonian and to the methods used to solve for the ground state. We found that the $^1S_0$ pairing gap is only somewhat lower than that predicted by the simple BCS theory for densities corresponding to $k_F < 0.5$ fm^{-1}, but the polarization effects due to the bulk are very important at higher densities, where a large suppression of the maximum value of the gap with respect to the BCS prediction was found. In particular, the maximum value of the gap is a bit larger with respect to other recent calculations and much larger than other calculations based on effective interactions.

ACKNOWLEDGMENTS

We thank A. Gezerlis, J. Carlson, J. Margueron, and C. Pethick for useful discussions. Calculations were partially performed on the BEN cluster at ECT* in Trento, under a grant for supercomputing projects, partially on the HPC facility "WIGLAF" of the Department of Physics, University of Trento, and partially on the HPC facility of SISSA/Democritos in Trieste. This work was supported in part by the NSF Grant PHY-0757703.

APPENDIX A: BCS WAVE FUNCTION PROJECTED TO FIXED N

The original BCS wave function was not an eigenstate of a particle number, i.e., it explicitly broke gauge symmetry. For spin-singlet paired fermions with the pairs having total momentum zero, the BCS form can be written as

$$|\mathrm{BCS}\rangle \propto \prod_{\boldsymbol{k}} [u_k + v_k a^+_{\boldsymbol{k}\uparrow} a^+_{-\boldsymbol{k}\downarrow}]|0\rangle, \tag{A1}$$

where the $a^+_{\boldsymbol{k}s}$ is the fermion creation operator for a particle in the $\boldsymbol{k}$ wave vector and spin projection s state, with anticommutation relations

$$\{a_{\boldsymbol{k}s}, a^+_{\boldsymbol{k}'s'}\} = \delta_{\boldsymbol{k},\boldsymbol{k}'}\delta_{s,s'}. \tag{A2}$$

The u_k and v_k here are functions only of the magnitude, $k = |\boldsymbol{k}|$, and this spatial symmetry along with the fermion antisymmetry guarantees only singlet pairs.

For our Monte Carlo calculations, it is simpler to use the projection of this state onto a fixed number of particles, N, in a periodic simulation cell of side L. We write the antisymmetric position- and spin-projected states as

$$\begin{aligned}\mathcal{A}|\boldsymbol{r}_1, s_1, \boldsymbol{r}_2, s_2, \ldots \boldsymbol{r}_N, s_N\rangle &= \frac{1}{N!}\sum_{\text{permutations P}} (-1)^P |P(\boldsymbol{r}_1, s_1, \boldsymbol{r}_2, s_2, \ldots \boldsymbol{r}_N, s_N)\rangle \\ &= \frac{1}{\sqrt{N!}}\psi^+_{s_1}(\boldsymbol{r}_1)\psi^+_{s_2}(\boldsymbol{r}_2)\ldots\psi^+_{s_N}(\boldsymbol{r}_N)|0\rangle,\end{aligned} \tag{A3}$$

where P represents the permutation of the particle labels, and $(-1)^P$ is 1 (-1) for even (odd) permutations. The position and momentum creation operators are related by

$$a^+_{\boldsymbol{k}s} = \frac{1}{L^{3/2}}\int_{-L/2}^{L/2} dx \int_{-L/2}^{L/2} dy \int_{-L/2}^{L/2} dz e^{i\boldsymbol{k}\cdot\boldsymbol{r}}\psi^+_s(\boldsymbol{r}). \tag{A4}$$

The standard BCS state is usually normalized by choosing $|u_k|^2 + |v_k|^2 = 1$. Since we will be projecting out the part with N particles, even if we start with a normalized state, the projected part will no longer be normalized. There is then no advantage to taking a normalized state, and instead we divide by each of the u_k. If one or more are zero, it simply means that we should drop the 1 term for that k value since it is always

filled. We therefore take

$$|\mathrm{BCS}\rangle = \prod_{\boldsymbol{k}} \left[1 + \frac{v_k}{u_k} a^+_{\boldsymbol{k}\uparrow} a^+_{-\boldsymbol{k}\downarrow}\right] |0\rangle. \tag{A5}$$

The particle-projected BCS wave function is then

$$\begin{aligned}\Psi_{\mathrm{BCS}}(\boldsymbol{R}, S) &= \langle \boldsymbol{R}, S|\mathrm{BCS}\rangle \\ &= \frac{1}{\sqrt{N!}} \langle 0|\psi_{s_N}(\boldsymbol{r}_N)\psi_{s_{N-1}}(\boldsymbol{r}_{N-1})\ldots\psi_{s_1}(\boldsymbol{r}_1) \\ &\quad \times \prod_{\boldsymbol{k}} \left[1 + \frac{v_k}{u_k} a^+_{\boldsymbol{k}\uparrow} a^+_{-\boldsymbol{k}\downarrow}\right] |0\rangle. \end{aligned} \tag{A6}$$

This is readily evaluated using Wick's theorem [53] to change from the given order to the normal order. Contracting $\psi_s(\boldsymbol{r})$ and $a^+_{\boldsymbol{k}s}$ gives

$$\overbrace{\psi_s(\boldsymbol{r})a^+_{\boldsymbol{k}s'}} = L^{-3/2} e^{i\boldsymbol{k}\cdot\boldsymbol{r}} \delta_{ss'}. \tag{A7}$$

From Eq. (A6), we see that either both $a^+_{\boldsymbol{k}\uparrow}$ and $a^+_{-\boldsymbol{k}\downarrow}$ in a pair or neither must be contracted with $\psi_s(\boldsymbol{r})$ operators to give a nonzero result. One particular contraction occurs when $\psi_{s_1}(\boldsymbol{r}_1)$ and $\psi_{s_2}(\boldsymbol{r}_2)$ contract with such a pair in $\boldsymbol{k}_1$, $\psi_{s_3}(\boldsymbol{r}_3)$ and $\psi_{s_4}(\boldsymbol{r}_4)$ contract with another pair in $\boldsymbol{k}_2$, etc. This gives a term

$$\begin{aligned}&\frac{v_{k_1}}{u_{k_1}} e^{i\boldsymbol{k}_1\cdot(\boldsymbol{r}_1-\boldsymbol{r}_2)} \langle s_1 s_2|\uparrow\downarrow\rangle \frac{v_{k_2}}{u_{k_2}} e^{i\boldsymbol{k}_2\cdot(\boldsymbol{r}_3-\boldsymbol{r}_4)} \langle s_3 s_4|\uparrow\downarrow\rangle \cdots \\ &\frac{v_{k_{N/2}}}{u_{k_{N/2}}} e^{i\boldsymbol{k}_{N/2}\cdot(\boldsymbol{r}_{N-1}-\boldsymbol{r}_N)} \langle s_{N-1} s_N|\uparrow\downarrow\rangle,\end{aligned} \tag{A8}$$

where we drop an unimportant overall normalization factor. Choosing different $\boldsymbol{k}$ terms to contract with corresponds to summing over all values of the $\boldsymbol{k}_1$, $\boldsymbol{k}_2$, etc., with the constraint that no two of the $\boldsymbol{k}_n$ values should be equal (anticommutating two pairs of operators does not change the sign). Choosing other contractions completely antisymmetrizes this form, and we can then include all terms in the $\boldsymbol{k}$ sums since these cancel when antisymmetrized. The result is

$$\Phi_{\mathrm{BCS}} = \mathcal{A}\left[\phi(\boldsymbol{r}_1, s_1, \boldsymbol{r}_2, s_2)\ldots\phi(\boldsymbol{r}_{N-1}, s_{N-1}, \boldsymbol{r}_N, s_N)\right], \tag{A9}$$

where for spin-singlet zero-momentum pairs,

$$\phi(\boldsymbol{r}_1, s_1, \boldsymbol{r}_2, s_2) = \sum_{\boldsymbol{k}} \frac{v_k}{u_k} e^{i\boldsymbol{k}\cdot(\boldsymbol{r}_1-\boldsymbol{r}_2)} \left[\langle s_1 s_2|\uparrow\downarrow\rangle\right]. \tag{A10}$$

Since the many-body antisymmetrizer will interchange the particles in ϕ, we usually explicitly antisymmetrize ϕ. We then get, up to an unimportant normalization,

$$\begin{aligned}&\phi(\boldsymbol{r}_1, s_1, \boldsymbol{r}_2, s_2) \\ &\quad = \sum_{\boldsymbol{k}} \frac{v_k}{u_k} e^{i\boldsymbol{k}\cdot(\boldsymbol{r}_1-\boldsymbol{r}_2)} \left[\langle s_1 s_2|\uparrow\downarrow\rangle - \langle s_1 s_2|\downarrow\uparrow\rangle\right],\end{aligned} \tag{A11}$$

which explicitly demonstrates the singlet pairing. For a very large simulation cell, the spatial function would be spherically symmetric and therefore an S state. For the typical sizes of our simulation cells, the function has the symmetry of the cube as seen in Fig. 6. Other possible fully paired states have different $\phi(\boldsymbol{r}_1, s_1, \boldsymbol{r}_2, s_2)$, but still have the general form of Eq. (A9).

Often we want to investigate systems that are not fully paired. Obviously, if we have an odd number of particles, at least one must be unpaired. We include unpaired particles in specific states by multiplying the $|\mathrm{BCS}\rangle$ state by a product of creation operators (or linear combinations of creation operators) for those states. The only change to the particle number projection described above is that these creation operators must be contracted with one of the $\psi_s(\boldsymbol{r})$ or the result will be zero. For n pairs and o occupied single-particle states, we have

$$\Phi_{\mathrm{BCS}} = \mathcal{A}[\phi_{12}\phi_{34}\ldots\phi_{2n-1,2n}\psi_1(2n+1)\ldots\psi_o(N)], \tag{A12}$$

which is Eq. (14).

APPENDIX B: PFAFFIAN CALCULATIONS

Here we give some details on how to calculate the Pfaffian. Proofs of the statements are given in Ref. [41]. The Pfaffian of a skew-symmetric matrix has the following three properties:

(i) Multiplying a row and the corresponding column by a constant is equivalent to multiplying the Pfaffian by a constant.
(ii) Interchanging two different rows and the corresponding columns changes the sign of the Pfaffian.
(iii) A multiple of a row and corresponding column added to another row and corresponding column does not change the value of the Pfaffian.

In addition, the matrix must have an even rank for the Pfaffian to be nonzero. Using these properties, it is straightforward to use, for example, Gauss elimination to reduce the skew-symmetric matrix to a block diagonal form with 2×2 blocks, whose Pfaffian is just the product of the nonzero elements in the first superdiagonal. A Fortran fragment showing the algorithm without pivoting for a complex matrix a of even rank n, is

```
p = (1.0, 0.0)
do i = 1, n, 2
do j = i + 2, n
fac = −a(i, j)/a(i, i + 1)
a(i + 1 : n, j) = a(i + 1 : n, j) + fac ∗ a(i + 1 : n, i + 1)
a(j, i + 1 : n) = a(j, i + 1 : n) + fac ∗ a(i + 1, i + 1 : n)
enddo
p = p ∗ a(i, i + 1)
enddo
```

As in standard Gauss elimination, we search the current row for a large pivot element, and pivot using property b to bring this onto the superdiagonal so that we do not divide by small numbers a(i,i + 1).

At the same time, we calculate the inverse of the matrix.

When one particle changes position or spin (or for calculation of one-body properties such as the gradient, kinetic energy, or expectation of a spin operator), the skew-symmetric matrix A has one row and the corresponding column changed. Writing the matrix B to be equal to A except for the row k with new elements B_{kj} and the corresponding column elements, Cayley

showed [54] that

$$\mathrm{Pf}[B] = \mathrm{Pf}[A] \sum_j B_{kj} A^{-1}_{jk}. \quad \text{(B1)}$$

For efficient algorithms with spin-dependent potentials, we want to be able to change two particles. A straightforward implementation would first change one row of the matrix as above and calculate the new Pfaffian, and update the inverse. Then change the corresponding column to obtain the skew-symmetric matrix and its inverse (its determinant is the square of the Pfaffian obtained before). This will require $O(N^2)$ operations. For each of the N second particles, we will require $O(N)$ operations to calculate the new Pfaffian if the first column is different for each pair. Unfortunately the result is $O(N^4)$ to calculate pairwise potentials.

However, for our case, the operation needed on a column or row is independent of the other column or row (except for the common element). We can therefore imagine doing a single update for particle 1 and using this for all the terms where the pair contains particle 1. The common element does not require an update and can be done separately.

It is most efficient to write this as a set of matrix multiplies. We define the new column j of the matrix to be C_{ij}, corresponding to a spin or derivative operator on particle j. Defining

$$P_{ij} = \sum_k A^{-1}_{ik} C_{kj},$$
$$G_{ij} = \sum_{mk} C^T_{im} A^{-1}_{mk} C_{kj} = \sum_m C_{mi} P_{mj} = -G_{ji}, \quad \text{(B2)}$$

we find that the ratio of the new to old Pfaffians with the two rows and columns denoted by i and j changed is

$$\frac{\mathrm{Pf(new)}}{\mathrm{Pf(old)}} = A^{-1}_{ji}\left[A^{\mathrm{new}}_{ij} + G_{ij}\right] + P_{ii}P_{jj} - P_{ij}P_{ji}, \quad \text{(B3)}$$

where A^{new} is the A matrix with new rows and columns.

[1] C. Pethick and D. Ravenhall, Annu. Rev. Nucl. Part. Sci. **45**, 429 (1995).
[2] H. Heiselberg and V. Pandharipande, Annu. Rev. Nucl. Part. Sci. **50**, 481 (2000).
[3] V. Stoks, R. Timmermans, and J. J. de Swart, Phys. Rev. C **47**, 512 (1993).
[4] S. Gandolfi, A. Y. Illarionov, S. Fantoni, F. Pederiva, and K. E. Schmidt, Phys. Rev. Lett. **101**, 132501 (2008).
[5] K. E. Schmidt and S. Fantoni, Phys. Lett. **B446**, 99 (1999).
[6] J. B. Anderson, J. Chem. Phys. **63**, 1499 (1975).
[7] J. Carlson, Phys. Rev. C **36**, 2026 (1987).
[8] S. C. Pieper, Nucl. Phys. **A751**, 516 (2005).
[9] S. Gandolfi, F. Pederiva, S. Fantoni, and K. E. Schmidt, Phys. Rev. Lett. **99**, 022507 (2007).
[10] S. Gandolfi, F. Pederiva, S. Fantoni, and K. E. Schmidt, Phys. Rev. C **73**, 044304 (2006).
[11] S. Gandolfi, F. Pederiva, and S. a Beccara, Eur. Phys. J. A **35**, 207 (2008).
[12] A. Sarsa, S. Fantoni, K. E. Schmidt, and F. Pederiva, Phys. Rev. C **68**, 024308 (2003).
[13] S. Gandolfi, A. Y. Illarionov, K. E. Schmidt, F. Pederiva, and S. Fantoni, Phys. Rev. C **79**, 054005 (2009).
[14] S. Gandolfi, F. Pederiva, S. Fantoni, and K. E. Schmidt, Phys. Rev. Lett. **98**, 102503 (2007).
[15] B. Friedman and V. Pandharipande, Nucl. Phys. **A361**, 502 (1981).
[16] A. Akmal, V. R. Pandharipande, and D. G. Ravenhall, Phys. Rev. C **58**, 1804 (1998).
[17] J. Carlson, J. Morales, V. R. Pandharipande, and D. G. Ravenhall, Phys. Rev. C **68**, 025802 (2003).
[18] A. Schwenk and C. J. Pethick, Phys. Rev. Lett. **95**, 160401 (2005).
[19] B. Borasoy, E. Epelbaum, H. Krebs, D. Lee, and U.-G. Meissner, Eur. Phys. J. A **35**, 357 (2008).
[20] D. Lee, Prog. Part. Nucl. Phys. **63**, 117 (2009).
[21] E. Epelbaum, H. Krebs, D. Lee, and U.-G. Meissner, Eur. Phys. J. A **40**, 199 (2009).
[22] A. Gezerlis and J. Carlson, Phys. Rev. C **77**, 032801(R) (2008).
[23] T. Abe and R. Seki, Phys. Rev. C **79**, 054002 (2009).
[24] T. Abe and R. Seki, Phys. Rev. C **79**, 054003 (2009).
[25] J. Bardeen, L. N. Cooper, and J. R. Schrieffer, Phys. Rev. **108**, 1175 (1957).
[26] R. B. Wiringa, V. G. J. Stoks, and R. Schiavilla, Phys. Rev. C **51**, 38 (1995).
[27] R. B. Wiringa and S. C. Pieper, Phys. Rev. Lett. **89**, 182501 (2002).
[28] B. S. Pudliner, V. R. Pandharipande, J. Carlson, S. C. Pieper, and R. B. Wiringa, Phys. Rev. C **56**, 1720 (1997).
[29] B. S. Pudliner, V. R. Pandharipande, J. Carlson, and R. B. Wiringa, Phys. Rev. Lett. **74**, 4396 (1995).
[30] J. Fujita and H. Miyazawa, Prog. Theor. Phys. **17**, 360 (1957).
[31] S. C. Pieper, V. R. Pandharipande, R. B. Wiringa, and J. Carlson, Phys. Rev. C **64**, 014001 (2001).
[32] S. Gandolfi, Ph.D. thesis, University of Trento, Italy, 2007, arXiv:0712.1364 [nucl-th].
[33] R. Guardiola, in *Microscopic Quantum Many-Body Theories and Their Applications, Proceedings of a European Summer School Held at Valencia, Spain, 8–19 September 1997*, Lecture Notes in Physics Vol. 510, edited by J. Navarro and A. Polls (Springer, Berlin, 1998), p. 269.
[34] L. Mitas, in *Quantum Monte Carlo Methods in Physics and Chemistry*, edited by M. P. Nightingale and C. J. Umrigar (NATO Advanced Study Institute on QMC, Cornell University, Ithaca, NY, 1999), p. 247.
[35] J. Carlson, in *Quantum Monte Carlo Methods in Physics and Chemistry*, edited by M. P. Nightingale and C. J. Umrigar (NATO Advanced Study Institute on QMC, Cornell University, Ithaca, NY, 1999), p. 287.
[36] F. Pederiva, A. Sarsa, K. E. Schmidt, and S. Fantoni, Nucl. Phys. **A742**, 255 (2004).
[37] J. Carlson, S.-Y. Chang, V. R. Pandharipande, and K. E. Schmidt, Phys. Rev. Lett. **91**, 050401 (2003).
[38] S. Y. Chang, V. R. Pandharipande, J. Carlson, and K. E. Schmidt, Phys. Rev. A **70**, 043602 (2004).
[39] J. P. Bouchaud, A. Georges, and C. Lhuillier, J. Physique **49**, 553 (1988).

[40] A. Fabrocini, S. Fantoni, A. Y. Illarionov, and K. E. Schmidt, Phys. Rev. Lett. **95**, 192501 (2005).
[41] M. Bajdich, L. Mitas, L. K. Wagner, and K. E. Schmidt, Phys. Rev. B **77**, 115112 (2008).
[42] A. Fabrocini, S. Fantoni, A. Y. Illarionov, and K. E. Schmidt, Nucl. Phys. **A803**, 137 (2008).
[43] A. Gezerlis and J. Carlson (private communication).
[44] I. E. Lagaris and V. R. Pandharipande, Nucl. Phys. **A359**, 331 (1981).
[45] J. Wambach, T. L. Ainsworth, and D. Pines, Nucl. Phys. **A555**, 128 (1993).
[46] J. M. C. Chen, J. W. Clark, R. D. Davé, and V. V. Khodel, Nucl. Phys. **A555**, 59 (1993).
[47] H. J. Schulze, J. Cugnon, A. Lejeune, M. Baldo, and U. Lombardo, Phys. Lett. **B375**, 1 (1996).
[48] A. Schwenk, B. Friman, and G. E. Brown, Nucl. Phys. **A713**, 191 (2003).
[49] L. G. Cao, U. Lombardo, and P. Schuck, Phys. Rev. C **74**, 064301 (2006).
[50] J. Margueron, H. Sagawa, and K. Hagino, Phys. Rev. C **77**, 054309 (2008).
[51] K. Hebeler, A. Schwenk, and B. Friman, Phys. Lett. **B648**, 176 (2007).
[52] V. R. Pandharipande and R. B. Wiringa, Rev. Mod. Phys. **51**, 821 (1979).
[53] G. C. Wick, Phys. Rev. **80**, 268 (1950).
[54] A. Cayley, Journal für die reine angewandte Mathematik **38**, 93 (1849), reprinted in *The Collected Mathematical papers of Arthur Cayley* (Cambridge University Press, Cambridge, 1889), Vol. 2, p. 19.